

Describing spatiotemporal memory patterns using animal movement modelling

Peter R. Thompson^{1,*}, Andrew E. Derocher¹, Mark A. Edwards^{2,3},
and Mark A. Lewis^{1,4}

¹Department of Biological Sciences, University of Alberta,
Edmonton, AB, Canada

²Mammalogy Department, Royal Alberta Museum, Edmonton,
AB, Canada

³Department of Renewable Resources, University of Alberta,
Edmonton, AB, Canada

⁴Department of Mathematical and Statistical Sciences, University
of Alberta, Edmonton, AB, Canada

*Correspondence: pt1@ualberta.ca

1 Abstract

1. Spatial memory plays a role in the way animals perceive their environments, resulting in memory-informed movement patterns that are observable to ecologists. Developing mathematical techniques to understand how animals use memory in their environments allows for an increased understanding of animal cognition.
2. Here we describe a model that accounts for the memory of seasonal or ephemeral qualities of an animal's environment. The model captures multiple behaviors at once by allowing for resource selection in the present time as well as long-distance navigations to previously visited locations within an animal's home range.
3. We performed a set of analyses on simulated data to test our model, determining that it can provide informative results from as little as one year of discrete-time location data. We also show that the accuracy of model selection and parameter estimation increases with more location data.
4. This model has potential to identify cognitive mechanisms for memory in a variety of ecological systems where periodic or seasonal revisit patterns within a home range may take place.

1.1 Keywords

step selection function, cognitive map, spatial memory, grizzly bear, *Ursus arctos*, animal movement, hidden Markov model

2 Introduction

Animal movement modelling has rapidly emerged as a subfield of ecology (Nathan et al., 2008) due to advances in animal tracking (Skaug and Fournier, 2006) and computational technology (Kristensen et al., 2016). The products of these advances have been widely applied to conservation and management (Fortin et al., 2005; Graham et al., 2012; Gerber et al., 2019). These models allow ecologists to understand the size and shape of an animal's home range (Worton, 1989) as well as what habitat attributes animals prefer on a finer scale (Gaillard et al., 2010). To address the latter, ecologists have developed tools such as resource selection functions (RSFs; Boyce and McDonald, 1999) and step selection functions (SSFs; Fortin et al., 2005). These allow for inference on an individual's habitat preference in what is known as third-order selection (Johnson, 1980; Thurfjell et al., 2014). The fine temporal and spatial resolution of these models allows ecologists to draw inference about a variety of behavioral processes, such as how an animal's movement rates are affected by its environment (Avgar et al., 2016; Prokopenko et al., 2017) and how movement patterns change at different

temporal scales (Oliveira-Santos et al., 2016; Richter et al., 2020). And yet, even with the advances that have been made in animal movement modelling, some notable behavioral mechanisms are often not considered.

Spatial memory, defined by Fagan et al. (2013) as memory of the spatial configuration of one's environment, is one of the most important influences on animal movement patterns. Many well-known behavioral processes, such as home range emergence (Van Moorter et al., 2009), food caching (Clayton and Dickinson, 1998), and even migration (Bracis and Mueller, 2017; Merkle et al., 2019), require the ability to remember the spatial location of landmarks or regions. Animal species use spatial memory in different ways (Fagan et al., 2013), and the benefits an animal may receive from memory often depend on its environment (Mueller and Fagan, 2008; Mueller et al., 2011). Theory on animal cognition has proposed that animals encode this spatial information in their brain as a cognitive map (Tolman, 1948). Ecologists have proposed multiple theories for the structure of these maps, with debate arising over whether a spatially explicit Euclidean map or a network-based topological map is more accurate (Bennett, 1996; Sturz et al., 2006; Normand and Boesch, 2009; Asensio et al., 2011). The true structure of these cognitive maps in animals is still unclear and may vary in different animal species.

Many animals experience seasonal variation within their home ranges (Morey et al., 2007; Wiktander et al., 2001), suggesting that a memory of these timings would be beneficial to optimize foraging. A key tenet of optimal foraging theory is that animals move to maximize their metabolic intake, and when the animal does decide to move, the timing of departure and the animal's subsequent destination are both important (Charnov, 1976). For example, primates time their journeys to previously visited resource patches with optimal feeding conditions as a means to maximize energetic intake (Janmaat et al., 2006). Sharks display intra-population variation and plasticity in their partially migratory movements, highlighting the viability of these long-distance navigations as an efficient foraging tactic (Papastamatiou et al., 2013). These recursive movement patterns are nearly impossible without spatial (or spatiotemporal) memory, where the animal must recall its previous interactions with the environment and associate those events with both a location and a time (Fagan et al., 2013). Movement models that incorporate spatial memory can provide insight on how human-animal conflict (Buderman et al., 2018), habitat fragmentation (Marchand et al., 2017), and global warming (Mauritzen et al., 2001) affect memory-informed animals.

Attempts to model these revisitations have proposed cognitive maps with spatial and temporal components, but have neglected to make inference about the specific nature of these influences. While many such approaches exist (Dalziel et al., 2008; Avgar et al., 2013; Vergara et al., 2016; Harel and Nathan, 2018), a common and simple technique involves integrating cognitive maps into SSFs (Oliveira-Santos et al., 2016; Marchand et al., 2017). A notable example is the model developed by Schlägel and Lewis (2014), where cognitive maps are based on time since last visit for each point in space. It is proposed that animals will only be encouraged to revisit locations when they have not visited them recently, as seen in some ecological systems (Davies and Houston, 1981).

This model was used to draw inference from gray wolf (*Canis lupus*) movement patterns (Schlägel et al., 2017), but it does not provide detail on when animals choose to revisit portions of their home range. The model only considers the last visit to any point in space, disregarding any previous visits to that point. Time since last visit alone is insufficient to model the complex time-dependent spatial memory that inspires movement patterns described above, because waiting longer to revisit such locations may not always be beneficial for the animals (e.g., trees that lose their ripe fruit after too long).

Here we describe a model that mathematically estimates the timing and precision of these seasonally recursive movements, and thus can be used to model periodic revisit patterns within an animal’s home range (Fig. 1). We employ innovative model fitting techniques (Kristensen et al., 2016; Fischer and Lewis, 2020) brought about by advances in computational methods to detect patterns in animal location data. Our modelling framework characterizes the movement of simulated or real animals according to four hypotheses: (N) the null hypothesis, assuming random walk behavior; (R) the resource-only hypothesis, assuming animals move entirely according to local resource gradients without memory; (M) the memory-only hypothesis, assuming animals exhibit seasonal revisit patterns within their home range with a prescribed periodicity; and (RM) the resource-memory hypothesis, assuming animals are simultaneously influenced by local resources and spatial memory.

To test our model, we first simulated movement tracks according to the model’s prescribed rules on simulated environments, subsequently analyzing how sample size affects both model selection and parameter estimation. We found that even with data sizes equivalent to roughly one year of animal tracking data, the model accurately identified movement patterns consistent with the four different hypotheses and produced accurate parameter estimates. These results improved when tracks with more locations were simulated. We then fit the model to telemetry data from a population of Arctic grizzly bears (*Ursus arctos*) and performed the same simulation analysis with real landscape data and movement parameters estimated for the bears. These bears live in a harsh environment where food resources are seasonal (Edwards and Derocher, 2015) and sparsely distributed (Edwards et al., 2009). We found a heavy influence of spatiotemporal memory in the bears’ movement patterns, although we determined that more data may be required to analyze these populations than for simulated movements.

3 Materials and Methods

Here we introduce a new modelling framework based on step selection functions that accounts for periodic or seasonal revisitations by animals that forage on ephemeral resources (Fig. 1). We developed a nested structure of four models in discrete time and continuous space (see Table 1 for a summary of the parameters and models) to address our four alternative hypotheses (N, R, M, RM). Our model fitting process, made possible through advanced automatic differ-

entiation techniques, allows for further inference about the specific nature of these cognitive mechanisms. The novelty and complexity of the computational processes used to analyze animal location data with our model motivated multiple simulation-based studies to identify the statistical power and parameter estimability of our models.

3.1 Modelling framework

We fit a hidden Markov model (HMM) to animal movement data to incorporate for switching between stationary (or quasi-stationary) and non-stationary states. HMMs are a first-order Markov process, implying that the animal’s current state is entirely dependent on its most recent state. This approach is common in movement ecology due to the multitude of behavioral strategies observed in foraging animals (Morales et al., 2004; Jonsen et al., 2013).

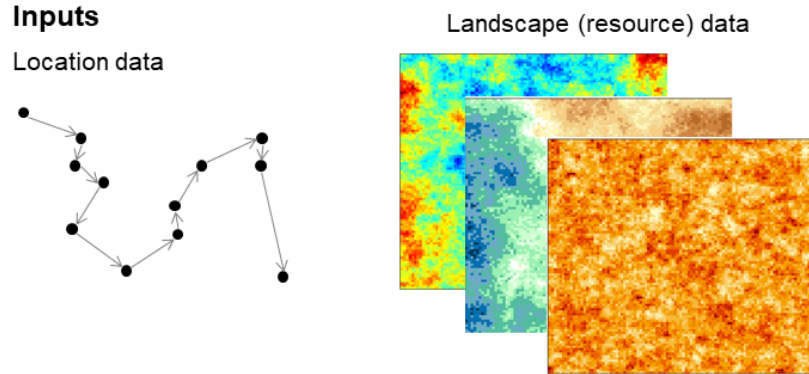
An HMM consists of a Markov matrix \mathbf{A} of state-switching probabilities as well as conditional probability distributions of the animal’s spatial location for each state (Jonsen et al., 2013). For a model with n different movement states, \mathbf{A} maps from $\mathbb{R}^n \rightarrow \mathbb{R}^n$, with each column summing to 1. Our model has two states, so we can infer the structure of \mathbf{A} from its diagonal. We denote these entries λ and γ , representing the probability that the animal will stay in the stationary or non-stationary state, respectively, given it was just there.

While our model is meant to be applied to continuous-space animal data, we make an approximation by discretizing our landscape over a two-dimensional square grid. Empirical landscape data is rarely continuous in space, and the resolution of this data can suggest a clear choice for the resolution of the domain grid. We assume that the boundaries of this grid are reflective, so if the animal reaches its edge, it will simply “bounce back” and remain on the grid. We define points in continuous space as x (or x_t to represent the animal’s location at time t) and their corresponding grid cells as z or z_t . Thus, $x_0 \in z_0$ is the animal’s initial location.

We define our conditional probability density functions for the stationary and non-stationary state f_s (which remains the same in all four models) and f_{ns} , respectively. Each conditional probability distribution represents a first-order Markov process modelling the animal’s location x_t and its bearing ϕ_t over time, which depend only on x_{t-1} and ϕ_{t-1} from the previous time step. Due to observation error in animal tracking data, we assumed that the animal’s observed location may change slightly even if it is not moving (Jonsen et al., 2013), so we allowed for small “movements” in our stationary state. The probability distribution for bearings in the stationary state, $g_s(\phi_t|\phi_{t-1})$, is a uniform distribution since we assume no directional autocorrelation here, so

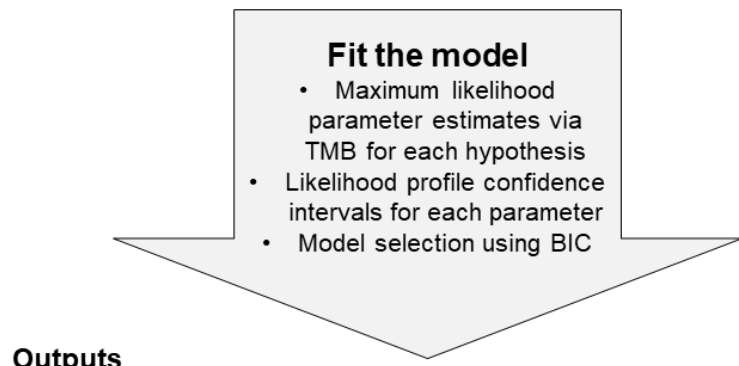
$$g_s(\phi_t|\phi_{t-1}) = \frac{1}{2\pi}, \quad (1)$$

$$f_s(x_t, \phi_t | x_{t-1}, \phi_{t-1}, \rho_s) = \frac{2}{\pi\sqrt{\rho_s}} g_s(\phi_t|\phi_{t-1}) \exp - \frac{\|x_t - x_{t-1}\|^2}{\pi\rho_s^2}. \quad (2)$$



4 Alternative Hypotheses → 4 Movement Models

Null	Resource-only
Animals move without regard to their external environments or memory	Animals move only according to local gradients in their environments
Memory-only	Resource-memory
Animals return to previously visited locations with repeated time lags	Animals select for local resources while also returning to resource-rich locations they previously visited



Outputs

- Explicit description of animal movement behavior via **parameter estimates** and **confidence intervals**
- Relative likelihood of each hypothesis via **BIC**

Figure 1: Schematic describing our modelling framework. Given an animal's movement track, quantified as a set of spatial coordinates, as well as landscape data describing an animal's environment, we fit four nested, competing models using maximum likelihood estimation. The insight we gain from this process allowed us to make conclusions about the mechanistic drivers of animal behavior.

When the animal is in the stationary state, the distance between x_t and x_{t-1} has a half-Gaussian distribution with mean ρ_s . The half-Gaussian distribution has thinner tails than the more traditionally used exponential distribution, decreasing the probability of longer movements from this state. We fix ρ_s to reduce model complexity, noting that it is fairly straightforward to do so based on the known degree of observation error or the resolution of environmental data.

In the non-stationary state, the animal may incorporate memory in its movements using a cognitive map (Tolman, 1948; Fig. 2). Our implementation of a cognitive map expands on the concept of time since last visit (Davies and Houston, 1981; Schlägel and Lewis, 2014; Schlägel et al., 2017) by allowing for the memory of more than just the last location to any point in space. Instead, we formulate the animal's cognitive map as the set of times since previous visits (TSPVs) for any area in space. This form of episodic-like memory, where animals remember a series of events with associated spatial locations and times, has been displayed in birds (Clayton and Dickinson, 1998) and great apes (Martin-Ordas et al., 2010). These animals can associate a point in space with an event (or set of events) and time (or set of times) when they visited there (Martin-Ordas et al., 2010). We define this map Z_t at each time t as a function over the domain grid. At each grid cell z , $Z_t(z)$ is a linked list of integers, with each element of the list representing an animal's visit to a point inside that cell. Z_0 is a grid full of empty linked lists, except for z_0 ; $Z_0(z_0)$ is a list with one element, 0. We can obtain Z_t if we know Z_{t-1} as well as the animal's location at time t . When t is incremented by 1, so is every entry on every linked list across the grid, and a new entry (0) is added to the linked list corresponding to the animal's new location:

$$Z_t(z) = \begin{cases} Z_{t-1}(z) + 1 & x_t \notin z \\ [Z_{t-1}(z) + 1, 0] & x_t \in z \end{cases}. \quad (3)$$

where $[Z_{t-1}(z) + 1, 0]$ implies adding 1 to every entry of the linked list $Z_{t-1}(z)$ and appending it with a new value 0.

The function f_{ns} , which models the animal's location and bearing in the non-stationary state, resembles a step selection function (Fortin et al., 2005), with two main components: k , the resource-independent movement kernel; and W , the environmental (or cognitive) weighting function. The function k describes the animal's locomotive capability while W , which may depend on the animal's cognitive map Z_{t-1} , describes how attractive the point is to the animal. This yields the following expression for f_{ns} :

$$\begin{aligned} f_{ns}(x_t, \phi_t | x_{t-1}, \phi_{t-1}, Z_{t-1}, \Theta_1, \Theta_2) \\ = \frac{k(x_t | x_{t-1}, \phi_{t-1}, \Theta_1)W(x_t | Z_{t-1}, \Theta_2)}{\int_{\Omega} k(x' | x_{t-1}, \phi_{t-1}, \Theta_1)W(x' | Z_{t-1}, \Theta_2)dx'}. \end{aligned} \quad (4)$$

The integral in the denominator serves as a normalization constant to ensure that f_{ns} integrates to 1. The parameter vector Θ_2 represents parameters related to the W and Θ_1 represents the locomotive parameters associated with

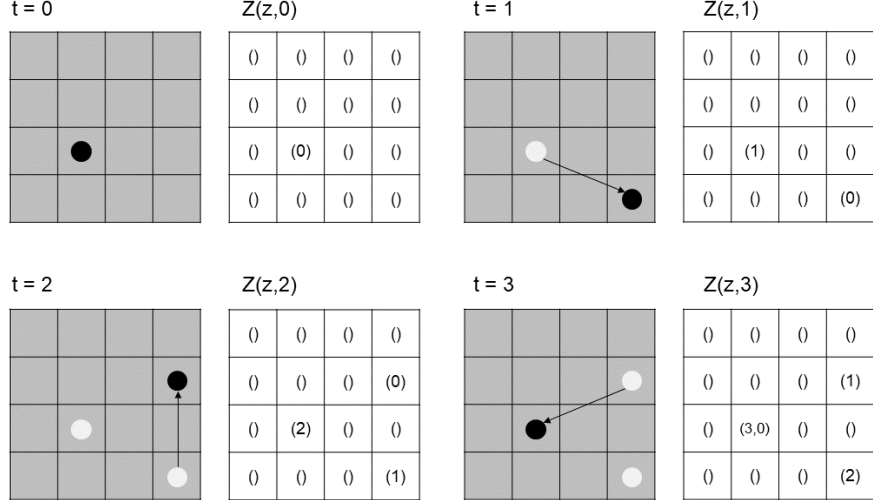


Figure 2: Diagram describing how an animal’s cognitive map Z changes over four discrete time steps, given an animal’s movement track, which is illustrated in the shaded panels. Each cell of Z contains a linked list that starts out empty but is iteratively appended as the animal traverses its environment.

k , namely ρ_{ns} which describes the animal’s mean step length and κ which describes the degree of directional autocorrelation in the animal’s movements. For each of our four models (null, resource-only, memory-only, resource-memory), the animal’s resource-independent movement kernel k has the same formulation. The distance between x_t and x_{t-1} , known as a step length, is exponentially distributed with mean parameter ρ_{ns} , and the bearing ϕ_t is von Mises distributed around ϕ_{t-1} with concentration parameter $\kappa \geq 0$ (Equation 5). Higher values of κ indicate straighter movement. We assume here that the animal’s step lengths and turning angles are independent. This modelling structure, known more generally as a correlated random walk, has been applied to a variety of ecological systems (Fortin et al., 2005; Codling et al., 2008; Auger-Méthé et al., 2015; Duchesne et al., 2015). We formulate k such that

$$g_{ns}(\phi_t | \phi_{t-1}) = \frac{\exp(\kappa \cos(\phi_t - \phi_{t-1}))}{2\pi I_0(\kappa)}, \quad (5)$$

$$k(x_t | x_{t-1}, \phi_{t-1}, \Theta_1) = \frac{\exp\left(-\frac{\|x_t - x_{t-1}\|}{\rho_{ns}}\right)}{\rho_{ns}} g_{ns}(\phi_t | \phi_{t-1}). \quad (6)$$

Notice that ϕ_t is not explicitly included in the left side of Equation 6; it can instead be calculated easily if x_t and x_{t-1} are known. If we denote $x_t =$

$(x_{t,1}, x_{t,2})^T \in \mathbb{R}^2$, then the following equation for ϕ_t holds:

$$\phi_t = \tan^{-1} \left(\frac{x_{t,2} - x_{t-1,2}}{x_{t,1} - x_{t-1,1}} \right) + \pi I(x_{t,1} < x_{t-1,1}), \quad (7)$$

where $I(x_{t,1} < x_{t-1,1})$ is an indicator function that is 1 if $x_{t,1} < x_{t-1,1}$ and 0 otherwise.

The only mathematical difference between the four models is the formulation of W . To differentiate between these different formulations, we refer to them as W_N , W_R , W_M , and W_{RM} for the null, resource-only, memory-only, and resource-memory models, respectively. The set of parameters we estimate in each model also varies, so we define $\Theta_{2,N}$, $\Theta_{2,R}$, $\Theta_{2,M}$, and $\Theta_{2,RM}$ in a similar respect.

3.1.1 Null model

The null model describes an animal's locomotive capability and directional autocorrelation based on its observed movement track. As a result, there is no extra weighting, so $W_N(x_t|Z_{t-1}, \Theta_{2,N}) = 1$ for all x_t in space, and $\Theta_{2,N}$ is the empty set. As a result, when considering the null model, f_{ns} is equal to k .

3.1.2 Resource-only model

The resource-only model has the following key component:

- (R1) the animal's movement is driven by third-order habitat selection in the present time within its immediate vicinity.

This modelling component also exists in RSFs (Boyce and McDonald, 1999) and SSFs (Fortin et al., 2005), which have received ample attention in movement ecology.

As a result, W_R resembles the weighting function from an SSF. If we are interested in P different resource covariates (expressed mathematically at each spatial location x as $r_1(x), \dots, r_P(x)$), we must estimate selection parameters β_1, \dots, β_P for each covariate. These parameters make up $\Theta_{2,R}$. The expression for our weighting function in the resource-only model is a linear combination of the covariates:

$$W_R(x_t|Z_{t-1}, \Theta_{2,R}) = \exp \left[\sum_{p=1}^P \beta_p r_p(x) \right]. \quad (8)$$

Notice that Z_{t-1} , the cognitive map, is not incorporated in the null or resource-only models since they do not include memory.

3.1.3 Memory-only model

The memory-only model contains the following key components:

- (M1) the animal uses a cognitive map to remember the timing of previous visits to regions of its environment, and
- (M2) it will return to locations it previously visited at a prescribed and scheduled time.

This type of cognitive map has been supported in the literature (Normand and Boesch, 2009; Martin-Ordas et al., 2010; Schlägel and Lewis, 2014) as has the validity of path recursions and revisititations as a foraging strategy for animals (Berger-Tal and Bar-David, 2015; Schlägel et al., 2017).

We calculate W_M based on distance to previously visited points on the animal's track. Given some time lag τ , we can use the cognitive map Z_t to find the point in space (or at least, the grid cell) where the animal was τ time indices ago. There is always exactly one grid cell $z_{t-\tau}$ where τ is an element of the linked list $Z_t(z_{t-\tau})$.

For each time lag τ , we compute the distance between the animal's current location and $z_{t-\tau}$, $\|x_t - z_{t-\tau}\|$, and transform it using an exponential decay function with decay parameter 10^α . α measures the order of magnitude on which the animal perceives its landscape spatially. Larger values of α indicate that the animal perceives its landscape to be more homogeneous. If α is larger, then $\exp(-10^\alpha \|x - y\|)$ is more likely to be small no matter how far apart the two points x and y are, suggesting that the animal cannot identify a difference between those distances. As α decreases, the mathematical difference between a step 1000 m away and a step 2000 m away is amplified, suggesting that the animal understands these differences in space on a wider scale.

The animal's periodic revisititation schedule, which is mediated by two parameters, dictates the weights for each of these exponentially transformed distances. The timing with which an animal navigates back to an existing location can be thought of as a random process, following a Gaussian distribution with mean parameter μ and standard deviation parameter σ . We can imagine that this timing reflects the state of the environment, with μ indicating the time scale at which resources may come and go and σ indicating the variability of these cycles. For any given time lag τ , the exponentially transformed distance between x_t and $z_{t-\tau}$ is weighted by the Gaussian probability distribution function $\varphi(\tau|\mu, \sigma)$. This produces a weighted mean of exponentially transformed distances, following the hypothesis that animals will navigate towards points they visited roughly μ time increments ago; the most "attractive" points for the animal are closest to z_μ . We introduce one final parameter, β_d , a "selection coefficient" for memorized locations. This parameter can be thought of as the relative probability of revisiting a memorized location instead of moving randomly or selecting for present-time resources. We restricted $\beta_d \geq 0.5$ (implying $\log \frac{\beta_d}{1-\beta_d} > 0$), in line with the hypothesis that animals select for (not against) previously visited locations.

The resulting formulation of W_M is as follows:

$$W_M(x_t|Z_{t-1}, \Theta_{2,M}) = \exp \left(\log \left(\frac{\beta_d}{1 - \beta_d} \right) \times \left[\frac{\sum_{\tau=1}^t \varphi(\tau|\mu, \sigma) \exp(-10^\alpha \|x_t - z_{t-\tau}\|)}{\sum_{\tau=1}^t \varphi(\tau|\mu, \sigma)} \right] \right). \quad (9)$$

3.1.4 Resource-memory model

The resource-memory model incorporates both resource selection and memory into the animal's movements, so (R1) and (M1) still remain as components in this model. However, there is one additional component that is not present in the resource-only or memory-only models:

- (RM1) the animal will return to locations it previously visited at a prescribed and scheduled time if habitat conditions there were favorable; otherwise it will avoid these areas.

Models combining resources and memory in some way have proven to be effective in explaining movement patterns for many different animals (Dalziel et al., 2008; Merkle et al., 2014; Schlägel et al., 2017).

The linear combination of resource covariates $\sum_{p=1}^P \beta_p r_p(x)$ is relative, so we introduced an additional parameter β_0 representing the relative probability of visiting a faraway location depending on its resource quality. If $\beta_0 = 1$ then the animal perceives all previously visited locations as “attractive” for revisitation. We transform this parameter with an inverse logistic function so it represents a pseudo-intercept (recall that traditional SSFs are conditional models and do not require an intercept; Fortin et al., 2005).

The weighting function now includes present-time resource selection in the first sum and memorized information in the second term:

$$W_{RM}(x_t|Z_{t-1}, \Theta_{2,RM}) = \exp \left(\sum_{p=1}^P \beta_p r_p(x_t) + \log \left(\frac{\beta_d}{1 - \beta_d} \right) \times \left[\frac{\sum_{\tau=1}^t \varphi(\tau|\mu, \sigma) \exp(-10^\alpha \|x_t - z_{t-\tau}\|) (\log \left(\frac{\beta_0}{1 - \beta_0} \right) + \sum_{p=1}^P \beta_p r_p(z_{t-\tau}))}{\sum_{\tau=1}^t \varphi(\tau|\mu, \sigma)} \right] \right). \quad (10)$$

The null model is a special case of both the resource-only and memory-only models, which are both a special case of the resource-memory model. Setting $\beta_i = 0$ for $i = 1, 2, \dots, P$ and $\log \left(\frac{\beta_0}{1 - \beta_0} \right) = 1$ in the resource-memory model yields the memory-only model, while setting $\beta_d = 0$ yields the resource-only model. Nesting models is advantageous for many mathematical reasons, including the ability to conduct likelihood ratio tests between models (Burnham and Anderson, 2004).

	Units	Description	N	R	M	RM
ρ_{ns}	$\frac{\text{distance}}{\text{time}}$	Mean movement speed in non-stationary state	X	X	X	X
κ	N/A	Degree of directional autocorrelation	X	X	X	X
β_0	N/A	Probability of revisitation				X
β_i	$\frac{1}{r_i \text{ units}}$	Resource selection coefficient(s)		X		X
β_d	N/A	Strength of selection for memorized areas			X	X
μ	time	Mean time lag between revisitations			X	X
σ	time	Standard deviation in time between revisitations			X	X
α	$\frac{1}{\text{distance}}$	Degree of perceptual resolution			X	X
λ	N/A	Probability of staying in stationary state	X	X	X	X
γ	N/A	Probability of staying in non-stationary state	X	X	X	X

Table 1: Description of model parameters, including units (N/A implies that the parameter is unitless) and models (N = null; R = resource-only; M = memory-only; RM = resource-memory) in which the parameters are estimated.

3.2 Statistical inference

We fit the four models to discrete-time, continuous-space animal movement data and used information theory to identify which corresponding hypothesis was most likely to be true. We identified the optimal set of parameters for a given track using maximum likelihood estimation, and used likelihood profiling to obtain accurate confidence intervals for our parameters.

3.2.1 Likelihood function

The likelihood of a set of model parameters for one step is a weighted sum of the conditional likelihood functions (f_s and f_{ns}), weighted by the probability of being in each state. These state probabilities depend on probabilities for the previous step, so for the first point we fit (there is no previous step), we fixed δ_s , the probability of being in the stationary state right before the data begins, as the proportion of steps shorter than ρ_s .

The likelihood function for the entire track is a product of the likelihoods for each step included in model fitting. We omitted all animal locations before some time t^* , since our model (or at least, the memory-only and resource-memory models) relies on past information to explain where the animal may go. We left the portion of the track that happened before $t = t^*$ to “train” the model on what the animal remembers. Thus, our iterative formula for the likelihood function begins at $t = t^*$. We define $\Phi_t \in \mathbb{R}^2$ as the vector of state probabilities for time $t \geq t^*$, and we calculate our likelihood using the iterative equations below:

$$\Phi_{t^*} = (\delta_s, 1 - \delta_s)^T, \quad (11)$$

$$\mathbf{P}_t = \begin{pmatrix} f_s(x_t | x_{t-1}, \rho_s) & 0 \\ 0 & f_{ns}(x_t, \phi_t | x_{t-1}, \phi_{t-1}, Z_{t-1}, \Theta_1, \Theta_2) \end{pmatrix}, \quad (12)$$

$$\Phi_t = \frac{\Phi_{t-1}^T \mathbf{P}_{t-1}}{\|\mathbf{P}_{t-1} \Phi_{t-1}\|} \mathbf{A}. \quad (13)$$

Then, following Whoriskey et al. (2017), the overall likelihood for the model is $\prod_{t=t^*}^{t_{max}} \Phi_t^T \mathbf{P}_t \mathbf{1}$, where $\mathbf{1} = (1, 1)^T$.

We approximate the denominator of Equation 4 with a sum so we do not have to integrate every time we evaluate the likelihood function. As is commonly done with SSFs (Thurfjell et al., 2014), we calculated W at a set of “control points” for each observed point x_t . If x_t , the endpoint of a step from x_{t-1} , is a random variable conditional on Z_{t-1} , Θ_1 , and Θ_2 , the integral in the denominator of Equation 4 is $E(W(x_t))$. Thus, we can approximate it by estimating the mean value of W at a set of simulated draws from x_t , which has probability density function k . This gives us the following approximation for f_{ns} :

$$\begin{aligned} \tilde{f}_{ns}(x_t, \phi_t | x_{t-1}, \phi_{t-1}, Z_{t-1}, \Theta_1, \Theta_2) \\ = \frac{k(x_t | x_{t-1}, \phi_{t-1}, \Theta_1) W(x_t | Z_{t-1}, \Theta_2)}{\frac{1}{K} \sum_{j=1}^K W(x_{t,j} | Z_{t-1}, \Theta_2)}, \end{aligned} \quad (14)$$

where $x_{t,j}$ represents the j^{th} control point (a simulated step starting at x_{t-1}) and K is the number of control points per observed step.

3.2.2 Fitting the model

We fit the model to data using maximum likelihood estimation, with the Template Model Builder (TMB) R package (Kristensen et al., 2016) improving numerical accuracy for this complex problem. TMB has been used to fit complex animal movement models, including HMMs (Albertsen et al., 2015; Auger-Méthé et al., 2017; Whoriskey et al., 2017). TMB uses automatic differentiation to calculate the gradient of a multidimensional likelihood function using pseudo-analytical methods, as opposed to traditional finite-difference methods that are slow and frequently result in numerical errors (Skaug and Fournier, 2006). We wrote a likelihood function for each model in C++, which TMB compiles and returns as a callable function in R (Kristensen et al., 2016). This allowed us to use an R optimizer of our choice while also benefiting from C++’s superior programming speed.

We used the R `nlminb` function to obtain maximum likelihood estimates for the negative log of our likelihood function. To prevent our model from producing errors or unrealistic results, we imposed various bounds on some of the parameters. We bounded the estimation for μ at t^* because if $\mu > t^*$, we would not be able to identify a signal due to a lack of training data. We also put

a lower bound on σ ; when this parameter was small, the partial derivative of our likelihood function with respect to μ became noisy, leading to computational errors in optimization. We found that a lower bound of approximately 20 time indices eliminated this problem. We additionally required estimates for $\alpha < -\log_{10}(\bar{\rho})$, where $\bar{\rho}$ is the animal's empirical mean step length (for context, we expect $\bar{\rho}$ to be close to but slightly smaller than ρ_{ns}). Values of α above this bound imply that the animal cannot perceive a difference between a few step lengths, which is unreasonable biologically. For parameters with fairly restrictive bounds (λ, γ, β_d , and β_0 , which are bounded between 0 and 1), we performed logit transformations ($\tilde{\lambda} = \log \frac{1}{1-\lambda}$, for example) so the optimizer would more effectively traverse the parameter space.

We tested two “initial values” for μ for each dataset we fit the model to, picking the fit that gave us the best likelihood function value. When profiling the likelihood surface with respect to this parameter, we often found many local optima, so we fit the model with initial values of t^* and $\frac{t^*}{2}$. This incurs additional computational time (we are effectively running the optimization algorithm twice) but is necessary due to the importance of picking a good initial value for each parameter (Pan and Wu, 1998). Using a different number of initial values for μ may be advantageous for some datasets.

For a model as complicated as this one, obtaining confidence intervals (CIs) using traditional Wald-type methods does not always produce accurate results. We frequently found this to be true for our model in practice so we used the likelihood profiling from Fischer and Lewis (2020). Given a multidimensional objective function with a known optimum, this algorithm finds confidence intervals for one parameter at a time by performing a binary search algorithm for a target function value (typically, the optimum minus some small confidence threshold). The algorithm starts searching at the optimal parameter value, and tries an initial step, fixing the parameter in question at this value and optimizing the rest of the function parameters. This process is repeated subsequently until the lengths of each step in parameter space are small enough for the algorithm to converge (Fischer and Lewis, 2020).

We used the Bayesian Information Criterion (BIC) to rank the four models by their likelihood and identify the hypothesis that was most likely to be true. BIC has a stronger penalization for model complexity than the more commonly used Akaike Information Criterion (AIC), and is a more useful criterion for model selection when one is interested in the truth of a hypothesis rather than the predictability of a model (Burnham and Anderson, 2004).

3.3 Simulation studies

Before applying our model to an ecological system, we simulated data and used it to test the model. These simulations are individual-based representations of our model that produce movement patterns associated with our four hypotheses. At each time index, we used our Markov matrix \mathbf{A} to decide whether the animal would change its behavioral state. If the animal was in the stationary state we simulated a random step from f_s (half-Gaussian step length, uniform turning

angle). For the non-stationary state, we simulated from f_{ns} using a Monte Carlo method (Parzen, 1961). We first calculated W for the entire grid, then we simulated a large number of random steps from k (Equations 5 and 6). This simulation process resembles the generation of control points in Equation 14, but we simulated $N_r = 10000$ steps at each point in time. Making N_r very large did not greatly affect computational time, so we did so in the interest of accurately approximating Equation 4. We then randomly choose one of the steps based on the values of W at each step, with the probability of any step $x_{t,i}$ being chosen described below:

$$\frac{W(x_{t,i}|Z_{t-1}, \Theta_2)}{\sum_{j=1}^{N_r} W(x_{t,j}|Z_{t-1}, \Theta_2)}. \quad (15)$$

For models that incorporate memory, we simulated memoryless training data ($W_M = W_N$ for the memory-only model, and $W_{RM} = W_R$ for the resource-memory model) for $t < t^*$. As expected, these initial points are omitted from model fitting.

3.3.1 Model verification: simulated data

We simulated tracks on artificial landscapes with preset model parameters, then fit the model to these tracks to explore parameter estimability and model selection accuracy. We varied the length of these tracks, $T = t_{max} - t^*$, as well as K , the number of controls points per step, to evaluate the amount of data required for accurate inference. Specifically, we tested four “treatment groups”: $T = 600, K = 10$; $T = 600, K = 50$; $T = 1200, K = 10$; and $T = 1200, K = 50$.

We used the R NLMR package (Sciaini et al., 2018) to simulate spatially autocorrelated Gaussian random fields representing our resource covariates. For each treatment group, we simulated 50 random movement tracks for each hypothesis. Each group of 50 tracks had the same set of parameters. In our simulations, we simulated environments for $P = 3$ resource covariates per track using the *nlm_gaussianfield* function in R. We then fit all four models to each track individually, then used BIC to identify how often the “correct” model was selected for each movement track. We compared these results with AIC to confirm that BIC is the most suitable information criterion for our modelling framework. We also estimated the bias and mean squared error (MSE; the mean squared difference between the parameter estimate and the true value) for each parameter with each model.

3.3.2 Model application: grizzly bear case study

We applied the model to grizzly bears in the Canadian Arctic, and then repeated the simulation study with data and model parameters from this system. Bears were captured from 2003 to 2006 and released with global positioning system (GPS) collars. Collars returned a location every four hours while the bear was not hibernating, and remained on the bears for up to four years (Edwards et al., 2009). The University of Alberta Animal Care and Use Committee for

Biosciences approved all animal capture and handling procedures, which were in accordance with the Canadian Council on Animal Care. The bears were collared in the Mackenzie River Delta region in the Northwest Territories (Edwards et al., 2009). Resources in the region are sparse and heterogeneous both in space and time (Shevtsova et al., 1995; Edwards and Derocher, 2015). To survive and forage optimally, bears take advantage of ephemeral, unpredictable, or seasonally available resources through a variety of foraging strategies (Edwards et al., 2009, 2011; Edwards and Derocher, 2015).

We analyzed grizzly bear habitat selection using multiple sources of environmental data describing the Mackenzie Delta region. Vegetation class data for the region assigned a one of 47 classes (indicating the dominant plant type or terrain) to each 30x30 m cell. A digital elevation model for the region (with 30x30 m cell resolution) provided information on elevation and slope. We also used an RSF layer estimating resource use for Arctic ground squirrels (*Urocitellus parryii*), a common grizzly bear prey item (Barker and Derocher, 2010; Edwards and Derocher, 2015). We considered $P = 6$ resource covariates: berry density, represented as a likelihood of having berries for each vegetation class; distance to turbid water, an indicator of broad whitefish (*Coregonus nasus*; a grizzly bear prey item; Barker and Derocher, 2009) density; Arctic ground squirrel density, taken directly from the RSF; sweetvetch (*Hedysarum alpinum*; a key grizzly bear food item; Edwards and Derocher, 2015) density, estimated by the vegetation class data; distance to the nearest of two towns in the region; and distance to six remote industrial camps (likely with little human activity).

Of the 21 bears with enough data for model fitting (at least two years of GPS collar data), we selected the eight with the most GPS fixes (these bears had at least three years of collar data). We set $\rho_s = 30$ meters, corresponding to the length of one grid cell for the environmental raster data, and we set $t^* = 365$ days. We used $K = 50$ control points when fitting the models. For each of these bears, we fit the models to the entire track as well as each year individually, comparing model selection between years. We then replicated that analysis using simulated bear tracks; for each bear, we simulated 100 movement tracks using the optimal parameters for each bear and the Mackenzie Delta environmental data. We simulated tracks of length $T = 600$ (approximately one year of grizzly bear GPS data, accounting for missed fixes and hibernation) and $T = 1200$ to evaluate how model selection accuracy changed with sample size. We used BIC to identify the hypothesis that most accurately explained each movement track, and also conducted likelihood ratio tests for each pair of nested models to determine the significance of specific behavioral signals.

4 Results

Our modelling structure allows ecologists to explain movement patterns identified from location data according to a set of four hypotheses, of which two incorporate complex time-dependent spatial memory. For animals that appear to use memory, our parametric approach evaluates the timing and precision of

navigations to previously visited locations in an animal’s home range. By fitting the model to simulated data we showed that the accuracy of the model is improved by sample size, and ecologists can also increase parameter estimability by simulating additional control points. Still, the amount of data required to draw accurate inference from the model is not large, as we show both with simulated environments and real-life landscape data (where the model is slightly less accurate).

4.1 Model verification: simulated data

The model’s ability to accurately characterize each type of movement behavior increased with the amount of location data (T) but not with the number of control points (K ; Table 2). The model identified null and resource-only movements accurately at all treatment levels, but the model’s ability to identify memory-only and resource-memory movement increased for longer simulated tracks. As a whole, increasing K does not improve model selection accuracy for either choice of T . The most common misidentification at all sample sizes was mistaking resource-memory movement for resource-only or memory-only movement.

		$K = 10$				$K = 50$			
		N	R	M	RM	N	R	M	RM
$T = 600$	N	48	0	0	2	47	0	0	3
	R	0	45	0	5	0	46	0	4
	M	7	0	40	3	4	0	44	2
	RM	0	5	7	38	0	8	7	35
$T = 1200$	N	49	0	0	1	45	0	0	5
	R	0	46	0	4	0	47	0	3
	M	2	0	47	1	0	0	50	0
	RM	0	3	2	45	0	7	2	41

Table 2: Breakdown of model selection counts using BIC for the simulated tracks. The row represents the “true” model that the tracks were simulated from (N = null; R = resource-only; M = memory-only; RM = resource-memory), while the column represents the model that was identified as the most parsimonious explanation of the data using BIC. Treatment groups are identified by the outer left and upper portions of the table and are separated by shading.

Using AIC instead of BIC resulted in a higher rate of “false positives” for memory (i.e., the resource-memory or the memory-only model was identified as the most parsimonious explanation for memoryless simulated tracks), and made model selection less accurate overall (Appendix: Table S1). Likelihood ratio tests on the same dataset for each pair of nested models revealed a similar trend; the likelihood ratio test often identified memory when it was not incorporated into the simulated tracks (Appendix: Table S2).

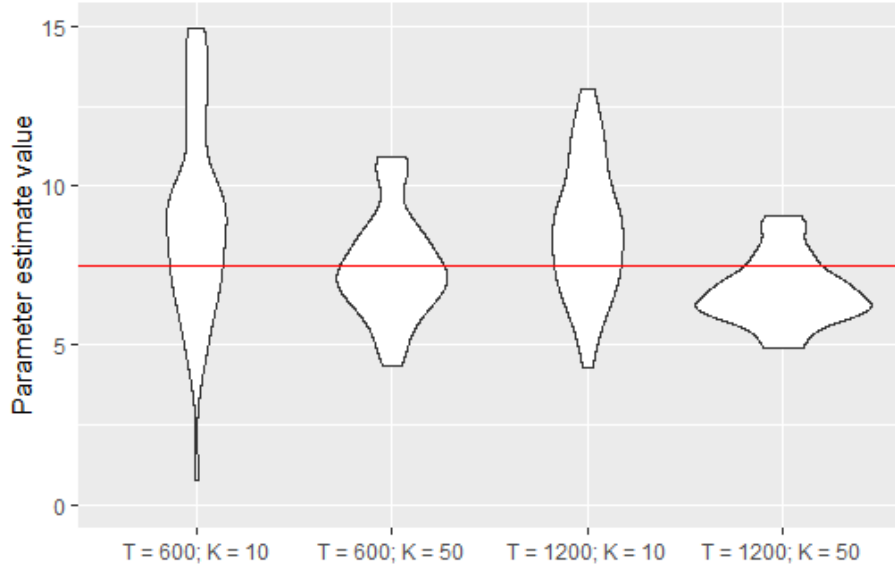


Figure 3: Violin plot of parameter estimates for β_1 in the resource-memory model for our four treatment groups (listed on the x-axis), with 50 simulations per plot. The true value of 7.5 is denoted by a horizontal red line.

The model produced more accurate parameter estimates with larger values of T and K (Table 3). When focusing on β_1 in the resource-memory model, we can see that bias does not change as much with different treatment groups as MSE (Fig. 3). For the simpler movement parameters ($\rho_{ns}, \kappa, \lambda, \gamma$), parameter estimates were consistent even with smaller values of T and K (Table 3).

4.2 Model application: grizzly bear case study

Memory played a significant part in the movements of five of the eight bears in the population (Table 4). When the data were broken up into one-year increments, model selection results varied annually, and sometimes differed even from the full dataset. For three of the bears (GF1008, GF1016, GM1046), the model identified as most explanatory of the bears' movement behaviors by BIC was different for the full dataset, the first subset, and the second subset. The resource-memory model was the most parsimonious explanation of the movement patterns of four bears, while the resource-only (2), memory-only (1), and null (1) models were also identified as most parsimonious in some cases. Four of the five memory-informed bears exhibited seasonal memory timescales close to one year ($\mu > 320$ days), while GF1016 had a μ value of 3 days. The six bears with resource selection included in their “best model” displayed similar resource selection patterns: significant selection for areas indicative of berries and Arctic

	True value	$T = 600$		$T = 1200$		$T = 600$		$T = 1200$	
		$K = 10$		$K = 10$		$K = 50$		$K = 50$	
		Bias	MSE	Bias	MSE	Bias	MSE	Bias	MSE
ρ_{ns}	0.75	-0.17	0.03	-0.18	0.04	-0.14	0.03	-0.17	0.04
κ	0.75	-0.21	0.05	-0.21	0.05	-0.19	0.04	-0.19	0.04
β_0	0.50	0.06	0.12	0.04	0.12	0.13	0.11	0.18	0.12
β_1	7.5	1.3	10.1	1.6	13.4	0.0	2.6	-0.7	1.7
β_2	-7.5	-1.2	7.8	-1.1	5.5	0.2	3.8	0.5	1.5
β_3	0.0	-0.1	5.0	0.4	4.3	-0.1	2.5	0.0	1.7
β_d	0.999	-0.04	0.02	-0.04	0.02	-0.01	0.00	-0.03	0.02
μ	500	-8	795	-13	543	-22	7819	-25	7277
σ	25	2	341	-3	32	1	197	-1	217
α	-1.78	-0.45	2.64	-0.28	1.30	-0.14	1.81	-0.67	2.17
λ	0.85	-0.02	0.001	-0.02	0.001	-0.02	0.002	-0.03	0.001
γ	0.90	-0.03	0.001	-0.03	0.001	-0.03	0.001	-0.03	0.001

Table 3: Estimates of bias and MSE for each parameter in the resource-memory model, averaged from 50 simulated movement tracks per treatment group. True values for each parameter are displayed on the left.

ground squirrels, avoidance of areas indicative of sweetvetch, and indifference to towns and cabins.

Bear ID	Full data	First subset	Second subset
GF1004	Resource-memory	Null	Resource-memory
GF1008	Resource-memory	Resource-only	Null
GF1016	Memory-only	Null	Resource-only
GF1041	Resource-memory	Resource-only	Resource-memory
GF1086	Resource-only	Resource-only	Resource-memory
GF1107	Resource-only	Resource-only	Resource-memory
GF1130	Null	Resource-memory	Null
GM1046	Resource-memory	Resource-only	Memory-only

Table 4: Model selection results for each bear in the Mackenzie Delta population. We list the hypothesis identified by BIC as most likely to be true given the data for the full dataset, the first subset, and the second subset.

Our simulation study revealed that at smaller sample sizes, the model occasionally failed to identify memory from memory-informed simulated tracks, but this issue is remedied with double the data. An example was GF1008, where only 10 of the 100 simulated tracks were correctly identified as “resource-memory” movements at $T = 600$. With $T = 1200$, this improved to 89. When we used likelihood ratio tests to compare the resource-memory model with the resource-only model (a special case of the resource-memory model) for GF1008, we found that at $T = 600$, 76 of our 100 simulated tracks registered a p-value

below 0.05, indicating that the resource-memory model was significantly more explanatory than the resource-only model 76% of the time. With $T = 1200$, this increased to 95. We observed similar trends for the other three resource-memory bears (GF1004, GF1041, GM1046) but not as strongly. It should be noted that GF1008 had the smallest estimate for β_d (2.3) of these bears. When we performed BIC model selection on simulated tracks based on GF1086, a “resource-only” bear, a false memory signal was identified more frequently with larger T (from 4 to 12 out of 100). This trend was not replicated for GF1107, the other “resource-only” bear (decrease from 10 to 7).

5 Discussion

Our model builds on existing literature to identify unique behavioral and cognitive mechanisms from animal movement data. Using advanced computational techniques, this novel and complex modelling framework can provide statistical inference for a variety of ecological systems. Our simulation studies provided insight on the viability of the model for different amounts of data.

We formulated a model that expresses parameters with clear biological implications to aid in the interpretation of our results, but we had to do so carefully to ensure that these parameters could be estimated accurately. Finding a set of biologically meaningful parameters with low mean squared error (Table 3) required a degree of trial and error, especially for β_0 and β_d . We chose to express them in a way that makes sense both biologically (where they represent relative probabilities) and mathematically (where they can easily be estimated with less error). While we can redefine these parameters without actually changing our likelihood function, we made sure to define parameters that are easy to estimate and biologically meaningful.

Our results provided support for a positive effect of the amount of location data and control points on parameter estimation, with the number of control points having a negligible effect on model selection accuracy. However, at all treatment groups, parameter estimates were occasionally inaccurate (Fig. 3, Table 3), and the model occasionally mistook the movement mechanisms driving the simulated tracks (Table 2). These outliers may be due to the stochasticity of simulated movement tracks; for example, a resource-only simulated animal may happen to visit similar portions of its landscape at a coincidentally regular interval, which the model might mistake for memory-informed movement. Conversely, an animal following the “memory-only” rules may coincidentally visit locations that happen to be particularly high (or low) in specific resource values, resulting in the movement track being best explained by the resource-memory or even the resource-only model.

Increasing the number of observed animal locations (T) improved our results, but we are more encouraged by the positive effects of simulating additional control points (K). While increasing T may require such costly tasks as using longer-lasting tracking devices, re-capturing animals and equipping them with new tracking devices periodically, or increasing the temporal resolution of track-

ing devices, increasing K is easy to do post-hoc. While increasing K may not yield benefits as large as increasing T , the cost of increasing K is much smaller.

Our simulated tracks consistently underestimated ρ_{ns} and κ in the resource-only and resource-memory models (Table 3), which is an artifact of the way we simulated the data. In these models, the animal “chooses” a step from N_r proposed steps, which are simulated from k , which depends on ρ_{ns} and κ . Our simulated landscapes are spatially autocorrelated, so if the simulated animal found itself in a resource-rich patch, it would be very likely to stay put. These movements are also less directionally autocorrelated than would be suggested by κ for similar reasons. Using an integrated step selection function (Avgar et al., 2016) could remedy these issues but for our purposes, it adds additional complexity to the model and is not our primary concern.

Our estimates of bias and MSE for α did not consistently decrease with increases in the amount of location data or the number of control points, potentially because of an odd bimodal distribution of parameter estimates (Appendix: Fig. S1). The larger portion of this bimodal distribution is clearly centered around the true value of approximately -1.78 for all four treatment groups, but curiously the “second” mode, which appears to be centered around -4.5, seems to account for more of the estimates T and K increase. These smaller estimates for α would imply that the hypothetical organisms moving according to our simulation rules occasionally behave with a much wider understanding of their environment, which they perceive to be spatially heterogeneous. The exact cause of these patterns requires further investigation.

When we applied the analysis to field data, we notice that the model’s effectiveness, especially when it comes to identifying a memory signal, increased greatly with sample size. Our simulations revealed that the model may miss a memory signal with inadequate data, which could explain the disparity between subsets of the data in Table 4. While it is possible that grizzly bears, especially females that take on different reproductive roles in different years, would change their movement strategies between years, it is also likely that the model may have not had enough data to identify a memory signal in an individual year. With twice data, the simulations accurately identified memory more often, suggesting that the memory signals identified for the entirety of each bear’s track are legitimate.

We occasionally observed “false positives” (the model identified memory as a driver of movement from memoryless simulated data) that increased in longer animal tracks ($K = 1200$ vs. $K = 600$) when simulating tracks with the grizzly bear data. This trend may be an artifact of how the Mackenzie Delta landscape data influenced simulated tracks, since false positives were much less frequent in the simulation study with artificial landscapes. When comparing this result with the real-life subsetting for the bears, we saw examples of subsetted data registering memory when the full data set did not, but we also saw examples of the opposite.

Our modelling framework operates under the assumption that resources vary in time, forcing animals to exhibit seasonal movement patterns within their home ranges. We do not explicitly model temporal resource variation, instead

assuming that our resource covariates $r_i(x)$ are constant in time. Temporally varying resource data are difficult to obtain (for example, they were unavailable for the Mackenzie Delta region), and transforming our data with some periodic function of time (e.g., $\tilde{r}_i(x, t) = r_i(x)g(t)$) would either require arbitrary choices on our part or the addition of parameters to an already complex model. Instead, we model resource variation in time through the animal’s behavior; in a way, we assume that μ is informative about how long resources take to re-appear, and as a result how long animals take to return to them.

While we used grizzly bears as a case study, the model was designed to be general and can be applied to a variety of different systems. Many animals, including turkey vultures (*Cathartes aura*; Holland et al., 2017), black vultures (*Coragyps atratus*; Holland et al., 2017), caribou (*Rangifer tarandus*; Lafontaine et al., 2017), and eastern indigo snakes (*Drymarchon couperi*; Bauder et al., 2016), perform seasonal movements within their home ranges. For data with higher temporal resolution, it would be possible to model complex time-dependent recursive movements on a diel scale, since many animals exhibit repetitive day-to-day movements within their home range (Christiansen et al., 2016; Herbig and Szedlmayer, 2016). Collecting data at finer temporal resolutions would be beneficial for inference on memory-informed movement, assuming observation errors are accounted for. Even patrolling predators, which were modeled by Schlägel and Lewis (2014), could be modeled using our framework, although we may expect estimates for μ to be smaller than in the grizzly bears. Schlägel et al. (2017) displayed the importance of time since last visit for gray wolves, but insight on when exactly wolves deem parts of their home range “re-visitable” could be interesting. Of course, migration is also seasonal and predictable, and although it is typically difficult to obtain environmental data for an animal’s entire migratory route, spatial memory has been identified as a key driver of migration in many instances (Mueller and Fagan, 2008; Mueller et al., 2011; Fagan et al., 2013; Bracis and Mueller, 2017; Merkle et al., 2019). Fitting this model to migratory populations could provide insights on how to quantify or potentially even predict these mechanisms.

6 Conclusions

Our model uses patterns in animal movement data to obtain information on complex time-dependent spatial memory patterns. Made possible by advanced computational techniques, we expand on existing literature from animal movement modelling as well as animal cognition to generate a model that can be applied to a variety of ecological systems. The model can estimate the timing of periodic revisitation patterns observed in an animal, which is novel, and also allows for the interaction of present-time resource selection and memory-informed navigation. We verify our model fitting process using simulated data before testing its utility on GPS collar data from grizzly bears, finding that this very complex model can be effective without need for immense data collection. We hope to apply this model more broadly to animals with different

foraging strategies as a means to compare the nature of time-dependent memory mechanisms in different ecological systems.

7 Acknowledgements

PRT was funded by the Ashley and Janet Cameron Graduate Scholarship, with support from UAlberta North, as well as the Alberta Graduate Excellence Scholarship. PRT was also supported by a University of Alberta Master’s Recruitment Award as well as a University of Alberta Doctoral Recruitment Award. MAL gratefully acknowledges support from a Canada Research Chair and NSERC Discovery grant. The authors declare no conflict of interest.

8 Author contributions

PRT designed the analysis with recommendations from MAL, AED, and MAE. MAE and AED collected and supplied grizzly bear data. PRT wrote the draft of the manuscript. All authors have reviewed and provided modifications to the manuscript.

9 Data accessibility

We intend to upload grizzly bear movement data to Dataverse, which is available through the University of Alberta.

References

Albertsen, C. M., Whoriskey, K., Yurkowski, D., Nielsen, A., and Flemming, J. M. (2015). Fast fitting of non-gaussian state-space models to animal movement data via template model builder. *Ecology*, 96:2598–2604.

Asensio, N., Brockelman, W. Y., Malaivijitnond, S., and Reichard, U. H. (2011). Gibbon travel paths are goal oriented. *Animal Cognition*, 14(3):395–405.

Auger-Méthé, M., Albertsen, C. M., Jonsen, I. D., Derocher, A. E., Lidgard, D. C., Studholme, K. R., Bowen, W. D., Crossin, G. T., and Mills Flemming, J. (2017). Spatiotemporal modelling of marine movement data using template model builder (tmb). *Marine Ecology Progress Series*, 565:237–249.

Auger-Méthé, M., Derocher, A. E., Plank, M. J., Codling, E. A., Lewis, M. A., and Börger, L. (2015). Differentiating the Lévy walk from a composite correlated random walk. *Methods in Ecology and Evolution*, 6(10):1179–1189.

Avgar, T., Deardon, R., and Fryxell, J. M. (2013). An empirically parameterized individual based model of animal movement, perception, and memory. *Ecological Modelling*, 251:158–172.

Avgar, T., Potts, J. R., Lewis, M. A., and Boyce, M. S. (2016). Integrated step selection analysis: bridging the gap between resource selection and animal movement. *Methods in Ecology and Evolution*, 7(5):619–630.

Barker, O. E. and Derocher, A. E. (2009). Brown bear (*Ursus arctos*) predation of broad whitefish (*Coregonus nasus*) in the mackenzie delta region, northwest territories. *Arctic*, 62(3):312–316.

Barker, O. E. and Derocher, A. E. (2010). Habitat selection by arctic ground squirrels (*Spermophilus parryii*). *Journal of Mammalogy*, 91(5):1251–1260.

Bauder, J. M., Breininger, D. R., Bolt, M. R., Legare, M. L., Jenkins, C. L., Rothermel, B. B., and McGarigal, K. (2016). Seasonal variation in eastern indigo snake (*Drymarchon couperi*) movement patterns and space use in peninsular florida at multiple temporal scales. *Herpetologica*, 72(3):214–226.

Bennett, A. T. (1996). Do animals have cognitive maps? *Journal of Experimental Biology*, 199:219–224.

Berger-Tal, O. and Bar-David, S. (2015). Recursive movement patterns: review and synthesis across species. *Ecosphere*, 6(9).

Boyce, M. S. and McDonald, L. (1999). Relating populations to habitats using resource selection functions. *TREE*, 14(7):268–272.

Bracis, C. and Mueller, T. (2017). Memory, not just perception, plays an important role in terrestrial mammalian migration. *Proc Biol Sci*, 284(1855).

Buderman, F. E., Hooten, M. B., Alldredge, M. W., Hanks, E. M., and Ivan, J. S. (2018). Time-varying predatory behavior is primary predictor of fine-scale movement of wildland-urban cougars. *Mov Ecol*, 6:22.

Burnham, K. P. and Anderson, D. R. (2004). Multimodel inference. *Sociological Methods & Research*, 33(2):261–304.

Charnov, E. (1976). Optimal foraging, the marginal value theorem. *Theoretical Population Biology*, 9:129–136.

Christiansen, F., Esteban, N., Mortimer, J. A., Dujon, A. M., and Hays, G. C. (2016). Diel and seasonal patterns in activity and home range size of green turtles on their foraging grounds revealed by extended fastloc-gps tracking. *Marine Biology*, 164(1).

Clayton, N. S. and Dickinson, A. (1998). Episodic-like memory during cache recovery by scrub jays. *Nature*, 395(6699):272–274.

Codling, E. A., Plank, M. J., and Benhamou, S. (2008). Random walk models in biology. *J R Soc Interface*, 5(25):813–34.

Dalziel, B. D., Morales, J. M., and Fryxell, J. M. (2008). Fitting probability distributions to animal movement trajectories: using artificial neural networks to link distance, resources, and memory. *Am Nat*, 172(2):248–58.

Davies, N. and Houston, A. (1981). Owners and satellites: The economics of territory defence in the pied wagtail, *Motacilla alba*. *Journal of Animal Ecology*, 50(1):157–180.

Duchesne, T., Fortin, D., and Rivest, L. P. (2015). Equivalence between step selection functions and biased correlated random walks for statistical inference on animal movement. *PLoS One*, 10(4):e0122947.

Edwards, M., Derocher, A. E., Hobson, K., Branigan, M., and Nagy, J. (2011). Fast carnivores and slow herbivores: differential foraging strategies among grizzly bears in the canadian arctic. *Oecologia*, 165:877–889.

Edwards, M. A. and Derocher, A. E. (2015). Mating-related behaviour of grizzly bears inhabiting marginal habitat at the periphery of their north american range. *Behavioural Processes*, 111:75–83.

Edwards, M. A., Nagy, J. A., and Derocher, A. E. (2009). Low site fidelity and home range drift in a wide-ranging, large arctic omnivore. *Animal Behaviour*, 77(1):23–28.

Fagan, W. F., Lewis, M. A., Auger-Methe, M., Avgar, T., Benhamou, S., Breed, G., LaDage, L., Schlagel, U. E., Tang, W. W., Papastamatiou, Y. P., Forester, J., and Mueller, T. (2013). Spatial memory and animal movement. *Ecology Letters*, 16(10):1316–29.

Fischer, S. M. and Lewis, M. A. (2020). A robust and efficient algorithm to find profile likelihood confidence intervals. *ArXiv*, pages 1–18.

Fortin, D., Beyer, H., Boyce, M. S., Smith, D., Duchesne, T., and Mao, J. (2005). Wolves influence elk movements: Behavior shapes a trophic cascade in yellowstone national park. *Ecology*, 86(5):1320–1330.

Gaillard, J. M., Hebblewhite, M., Loison, A., Fuller, M., Powell, R., Basille, M., and Van Moorter, B. (2010). Habitat-performance relationships: finding the right metric at a given spatial scale. *Philos Trans R Soc Lond B Biol Sci*, 365(1550):2255–65.

Gerber, B. D., Hooten, M. B., Peck, C. P., Rice, M. B., Gammonley, J. H., Apa, A. D., Davis, A. J., and Lemaître, J. (2019). Extreme site fidelity as an optimal strategy in an unpredictable and homogeneous environment. *Functional Ecology*, 33(9):1695–1707.

Graham, R. T., Witt, M. J., Castellanos, D. W., Remolina, F., Maxwell, S., Godley, B. J., and Hawkes, L. A. (2012). Satellite tracking of manta rays highlights challenges to their conservation. *PLoS One*, 7(5):e36834.

Harel, R. and Nathan, R. (2018). The characteristic time-scale of perceived information for decision-making: Departure from thermal columns in soaring birds. *Functional Ecology*, 32(8):2065–2072.

Herbig, J. L. and Szedlmayer, S. T. (2016). Movement patterns of gray triggerfish, *Balistes capriscus*, around artificial reefs in the northern gulf of mexico. *Fisheries Management and Ecology*, 23(5):418–427.

Holland, A. E., Byrne, M. E., Bryan, A. L., DeVault, T. L., Rhodes, O. E., and Beasley, J. C. (2017). Fine-scale assessment of home ranges and activity patterns for resident black vultures (*Coragyps atratus*) and turkey vultures (*Cathartes aura*). *PLoS One*, 12(7):e0179819.

Janmaat, K. R., Byrne, R. W., and Zuberbuhler, K. (2006). Primates take weather into account when searching for fruits. *Curr Biol*, 16(12):1232–7.

Johnson, D. (1980). The comparison of usage and availability measurements for evaluating resource preference. *Ecology*, 61(1):65–71.

Jonsen, I. D., Basson, M., Bestley, S., Bravington, M. V., Patterson, T. A., Pedersen, M. W., Thomson, R., Thygesen, U. H., and Wotherspoon, S. J. (2013). State-space models for bio-loggers: A methodological road map. *Deep Sea Research Part II: Topical Studies in Oceanography*, 88-89:34–46.

Kristensen, K., Nielsen, A., Berg, C. W., Skaug, H., and Bell, B. M. (2016). TMB: Automatic differentiation and Laplace approximation. *Journal of Statistical Software*, 70(5).

Lafontaine, A., Drapeau, P., Fortin, D., and St-Laurent, M. H. (2017). Many places called home: the adaptive value of seasonal adjustments in range fidelity. *J Anim Ecol*, 86(3):624–633.

Marchand, P., Garel, M., Bourgoin, G., Duparc, A., Dubray, D., Maillard, D., and Loison, A. (2017). Combining familiarity and landscape features helps break down the barriers between movements and home ranges in a non-territorial large herbivore. *J Anim Ecol*, 86(2):371–383.

Martin-Ordas, G., Haun, D., Colmenares, F., and Call, J. (2010). Keeping track of time: evidence for episodic-like memory in great apes. *Anim Cogn*, 13(2):331–40.

Mauritzen, M., Derocher, A. E., and Wiig, Ø. (2001). Space-use strategies of female polar bears in a dynamic sea ice habitat. *Canadian Journal of Zoology*, 79(9):1704–1713.

Merkle, J. A., Fortin, D., and Morales, J. M. (2014). A memory-based foraging tactic reveals an adaptive mechanism for restricted space use. *Ecol Lett*, 17(8):924–31.

Merkle, J. A., Sawyer, H., Monteith, K. L., Dwinnell, S. P. H., Fralick, G. L., and Kauffman, M. J. (2019). Spatial memory shapes migration and its benefits: evidence from a large herbivore. *Ecol Lett*, 22(11):1797–1805.

Morales, J. M., Haydon, D. T., Frair, J., Holsinger, K. E., and Fryxell, J. M. (2004). Extracting more out of relocation data: Building movement models as mixtures of random walks. *Ecology*, 85(9):2436–2445.

Morey, P. S., Gese, E. M., and Gehrt, S. D. (2007). Spatial and temporal variation in the diet of coyotes in the Chicago metropolitan area. *The American Midland Naturalist*, 158(1):147–161.

Mueller, T. and Fagan, W. F. (2008). Search and navigation in dynamic environments - from individual behaviors to population distributions. *Oikos*, 117:654–664.

Mueller, T., Fagan, W. F., and Grimm, V. (2011). Integrating individual search and navigation behaviors in mechanistic movement models. *Theoretical Ecology*, 4(3):341–355.

Nathan, R., Getz, W., Revilla, E., Holyoak, M., Kadmon, R., Saltz, D., and Smouse, P. E. (2008). A movement ecology paradigm for unifying organismal movement research. *PNAS*, 105(49):19052–19059.

Normand, E. and Boesch, C. (2009). Sophisticated Euclidean maps in forest chimpanzees. *Animal Behaviour*, 77(5):1195–1201.

Oliveira-Santos, L. G., Forester, J. D., Piovezan, U., Tomas, W. M., and Fernandez, F. A. (2016). Incorporating animal spatial memory in step selection functions. *J Anim Ecol*, 85(2):516–24.

Pan, L. and Wu, L. (1998). A hybrid global optimization method for inverse estimation of hydraulic parameters: Annealing-simplex method. *Water Resources Research*, 34(9):2261–2269.

Papastamatiou, Y. P., Meyer, C. G., Carvalho, F., Dale, J. J., Hutchinson, M. R., and Holland, K. N. (2013). Telemetry and random-walk models reveal complex patterns of partial migration in a large marine predator. *Ecology*, 94(11):2595–2606.

Parzen, E. (1961). On estimation of a probability density function and mode. *The Annals of Mathematical Statistics*, 33:1065–1076.

Prokopenko, C. M., Boyce, M. S., Avgar, T., and Tulloch, A. (2017). Characterizing wildlife behavioural responses to roads using integrated step selection analysis. *Journal of Applied Ecology*, 54(2):470–479.

Richter, L., Balkenhol, N., Raab, C., Reinecke, H., Meißner, M., Herzog, S., Isselstein, J., and Signer, J. (2020). So close and yet so different: the importance of considering temporal dynamics to understand habitat selection. *Basic and Applied Ecology*, 43:99–109.

Schlägel, U. E. and Lewis, M. A. (2014). Detecting effects of spatial memory and dynamic information on animal movement decisions. *Methods in Ecology and Evolution*, 5(11):1236–1246.

Schlägel, U. E., Merrill, E. H., and Lewis, M. A. (2017). Territory surveillance and prey management: Wolves keep track of space and time. *Ecol Evol*, 7(20):8388–8405.

Sciajini, M., Fritsch, M., Scherer, C., Simpkins, C. E., and Golding, N. (2018). Nlmr and landscapetools: An integrated environment for simulating and modifying neutral landscape models in R. *Methods in Ecology and Evolution*, 9(11):2240–2248.

Shevtsova, A., Ojala, A., Neuvonen, S., Vieno, M., and Haukioja, E. (1995). Growth and reproduction of dwarf shrubs in a subarctic plant community: Annual variation and above-ground interactions with neighbours. *Journal of Ecology*, 83(2):263–275.

Skaug, H. J. and Fournier, D. A. (2006). Automatic approximation of the marginal likelihood in non-gaussian hierarchical models. *Computational Statistics & Data Analysis*, 51(2):699–709.

Sturz, B. R., Bodily, K. D., and Katz, J. S. (2006). Evidence against integration of spatial maps in humans. *Anim Cogn*, 9(3):207–17.

Thurfjell, H., Ciuti, S., and Boyce, M. S. (2014). Applications of step-selection functions in ecology and conservation. *Movement Ecology*, 2(4):1–12.

Tolman, E. C. (1948). Cognitive maps in rats and men. *The Psychological Review*, 55(4):189–208.

Van Moorter, B., Visscher, D., Benhamou, S., Börger, L., Boyce, M. S., and Gaillard, J.-M. (2009). Memory keeps you at home: a mechanistic model for home range emergence. *Oikos*, 118(5):641–652.

Vergara, P. M., Soto, G. E., Moreira-Arce, D., Rodewald, A. D., Meneses, L. O., and Perez-Hernandez, C. G. (2016). Foraging behaviour in Magellanic woodpeckers is consistent with a multi-scale assessment of tree quality. *PLoS One*, 11(7):e0159096.

Whoriskey, K., Auger-Methe, M., Albertsen, C. M., Whoriskey, F. G., Binder, T. R., Krueger, C. C., and Mills Flemming, J. (2017). A hidden Markov movement model for rapidly identifying behavioral states from animal tracks. *Ecol Evol*, 7(7):2112–2121.

Wiktander, U., Olsson, O., and Nilsson, S. J. (2001). Seasonal variation in home-range size, and habitat area requirement of the lesser spotted woodpecker (*Dendrocopos minor*) in southern sweden. *Biological Conservation*, 100:387–385.

Worton, B. (1989). Kernel methods for estimating the utilization distribution in home-range studies. *Ecology*, 70(1):164–168.

10 Appendix

		K = 10				K = 50			
		N	R	M	RM	N	R	M	RM
T = 600	N	20	7	2	21	27	4	3	16
	R	0	24	0	26	0	26	0	24
	M	3	0	24	23	0	0	25	25
	RM	0	2	5	43	0	0	2	48
T = 1200	N	28	1	1	20	29	2	1	18
	R	0	35	0	15	0	32	0	18
	M	0	0	15	35	0	0	20	30
	RM	0	0	1	49	0	0	0	50

Table S1: Breakdown of model selection counts using AIC for different types of simulated tracks. The row represents the “true” model that the tracks were simulated from (N = null; R = resource-only; M = memory-only; RM = resource-memory), while the column represents the model that was identified as the most parsimonious explanation of the data using AIC. Treatment groups are identified by the outer left and upper portions of the table and are separated by shading.

		K = 10					K = 50				
		N-R	N-M	N-RM	R-RM	M-RM	N-R	N-M	N-RM	R-RM	M-RM
T = 600	N	5	2	26	25	9	3	3	17	18	27
	R	50	24	50	22	50	50	22	50	20	50
	M	4	45	46	45	22	3	48	50	50	23
	RM	50	47	50	47	45	50	49	50	50	48
T = 1200	N	0	0	21	24	27	1	1	19	19	24
	R	50	31	50	13	50	50	29	50	16	50
	M	2	48	50	50	33	0	50	50	50	28
	RM	50	50	50	50	49	50	49	50	50	50

Table S2: Breakdown of likelihood ratio test results for different types of simulated tracks. The row represents the “true” model that the tracks were simulated from (N = null; R = resource-only; M = memory-only; RM = resource-memory), while the column represents the two models that were compared using a likelihood ratio test. Counts represent the number of simulated tracks (50 per cell) that registered a p-value below 0.05 for the indicated likelihood ratio test (for example, the “N-R” column indicates likelihood ratio tests determining whether the resource-only model is significantly more explanatory than the null model). Treatment groups are identified by the outer left and upper portions of the table and are separated by shading.

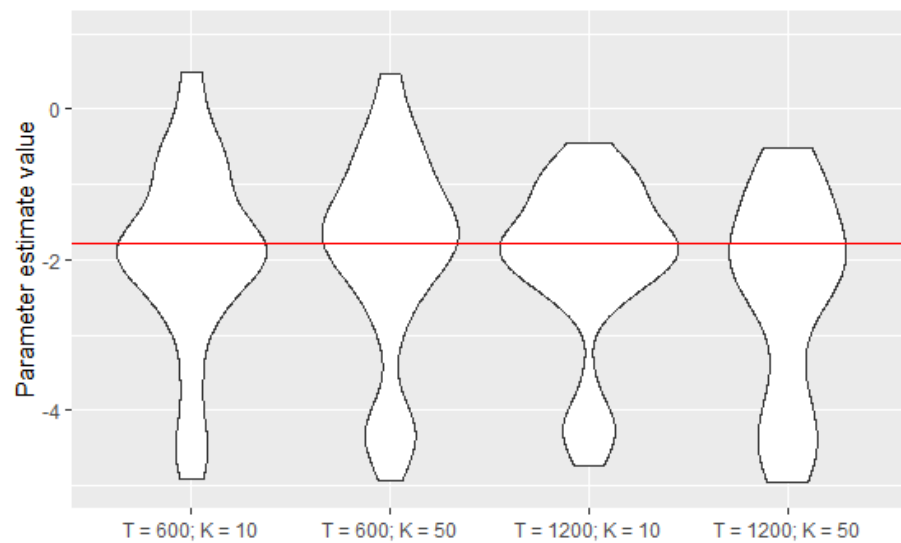


Figure S1: Violin plot of parameter estimates for α parameter in the resource-memory model for our four treatment groups (detailed on the x-axis), with 50 simulations per treatment. The true value of $\log_{10} \frac{1}{60} \approx -1.78$ is denoted by a horizontal red line.